

## Article

# Synthetic Circular RNA for microRNA-1269a Suppresses Tumor Progression in Oral Squamous Cell Carcinoma

Atsushi Kasamatsu <sup>1,\*</sup>, Ryunosuke Nozaki <sup>1</sup>, Kohei Kawasaki <sup>2</sup>, Tomoaki Saito <sup>2</sup>, Chikashi Minemura <sup>3</sup>, Naohiko Seki <sup>4</sup>, Joel Moss <sup>5</sup> and Katsuhiko Uzawa <sup>1,2,\*</sup>

<sup>1</sup> Department of Dentistry and Oral-Maxillofacial Surgery, Chiba University Hospital, 1-8-1 Inohana, Chuo-ku, Chiba-shi 260-8677, Chiba, Japan; nozaki.r@chiba-u.jp

<sup>2</sup> Department of Oral Science, Graduate School of Medicine, Chiba University, 1-8-1 Inohana, Chuo-ku, Chiba-shi 260-8670, Chiba, Japan; kou0802hei@gmail.com (K.K.); tomoakisaito@chiba-u.jp (T.S.)

<sup>3</sup> Department of Oral and Maxillofacial Surgery, National Defense Medical College Hospital, Tokorozawa 359-8513, Saitama, Japan; minichika.cm@gmail.com

<sup>4</sup> Department of Functional Genomics, Graduate School of Medicine, Chiba University, Chiba-shi 260-8670, Chiba, Japan; naoseki@faculty.chiba-u.jp

<sup>5</sup> Critical Care Medicine and Pulmonary Branch, National Heart, Lung, and Blood Institute, National Institutes of Health, Bethesda, MD 20892-1590, USA; mossj@nhlbi.nih.gov

\* Correspondence: kasamatsua@faculty.chiba-u.jp (A.K.); uzawak@faculty.chiba-u.jp (K.U.)

**Simple Summary:** Circular RNAs (circRNAs) are a new class of unique RNAs that have single-stranded, covalently closed, and continuous loop structures, which confer stability and resistance to endonuclease-mediated degradation that in turn affords substantially longer circulatory half-lives relative to linear RNAs. In this study, we established a novel synthetic circRNA that carries miR-1269a binding sequences and investigated its potential application as a therapeutic tool to slow cancer progression. Briefly, phospholipase C gamma 2 (PLCG2), which is related to oral squamous cell carcinoma (OSCC) clinical stage and overall survival, was affected by the circRNA-1269a/miR-1269a axis. Our confirmation that circRNA-1269a/miR-1269a/PLCG2 can inhibit OSCC proliferation and migration by promoting apoptosis in OSCC cells in vitro indicates that PLCG2 overexpression via the circRNA1269a/miR-1269a axis may be a valuable tool for controlling OSCC growth. Therefore, these data suggest that circRNA-1269a/miR-1269a could act as a potential therapeutic axis for OSCCs.



**Citation:** Kasamatsu, A.; Nozaki, R.; Kawasaki, K.; Saito, T.; Minemura, C.; Seki, N.; Moss, J.; Uzawa, K. Synthetic Circular RNA for microRNA-1269a Suppresses Tumor Progression in Oral Squamous Cell Carcinoma. *Cancers* **2024**, *16*, 1242. <https://doi.org/10.3390/cancers16061242>

Academic Editor: Daisuke Uchida

Received: 11 February 2024

Revised: 12 March 2024

Accepted: 18 March 2024

Published: 21 March 2024



**Copyright:** © 2024 by the authors. Licensee MDPI, Basel, Switzerland. This article is an open access article distributed under the terms and conditions of the Creative Commons Attribution (CC BY) license (<https://creativecommons.org/licenses/by/4.0/>).

**Abstract:** microRNAs (miRs) function in cancer progression as post-transcriptional regulators. We previously reported that endogenous circular RNAs (circRNAs) function as efficient miR sponges and could act as novel gene regulators in oral squamous cell carcinoma (OSCC). In this study, we carried out cellular and luciferase reporter assays to examine competitive inhibition of miR-1269a, which is upregulated expression in several cancers, by circRNA-1269a, a synthetic circRNA that contains miR-1269a binding sequences. We also used data-independent acquisition (DIA) proteomics and in silico analyses to determine how circRNA-1269a treatment affects molecules downstream of miR-1269a. First, we confirmed the circularization of the linear miR-1269a binding site sequence using RT-PCR with divergent/convergent primers and direct sequencing of the head-to-tail circRNA junction point. In luciferase reporter and cellular functional assays, circRNA-1269a significantly reduced miR-1269a function, leading to a significant decrease in cell proliferation and migration. DIA proteomics and gene set enrichment analysis of OSCC cells treated with circRNA-1269a indicated high differential expression for 284 proteins that were mainly enriched in apoptosis pathways. In particular, phospholipase C gamma 2 (PLCG2), which is related to OSCC clinical stage and overall survival, was affected by the circRNA-1269a/miR-1269a axis. Taken together, synthetic circRNA-1269a inhibits tumor progression via miR-1269a and its downstream targets, indicating that artificial circRNAs could represent an effective OSCC therapeutic.

**Keywords:** circRNA; artificial synthetic circRNA; microRNA; miR-1269a; phospholipase C gamma 2; squamous cell carcinoma

## 1. Introduction

microRNAs (miRs) are small non-coding RNAs that modulate translational repression or degradation of mRNA molecules by binding to 3' untranslated regions of target mRNAs [1]. miRs have been extensively understood in critical biological processes including tumor proliferation, apoptosis, and differentiation. Aberrant miR expression is linked closely to the initiation and progression of numerous cancers [2]. Therefore, disturbance of miRs can act as oncogenes (onco-miRs) or tumor suppressor genes (ts-miRs) and play critical roles in tumorigenesis and progression [2–5].

Circular RNAs (circRNAs) are a novel class of unique RNAs, characterized by single-stranded, covalently closed, and continuous loop structures [6]. circRNAs are produced by backsplicing or head-to-tail splicing of linear RNAs [7] to form covalently closed loop structures without 5'–3' polarity or a polyadenylated tail [6,8–11]. The loop structures of circRNAs confer stability and resistance to endonuclease-mediated degradation that in turn affords substantially longer circulatory half-lives relative to linear RNAs [12]. Endogenous circRNAs contain selectively conserved miR binding sites and thereby can function as efficient miR sponges that counteract miR activity [12–15]. Although recent research on circRNAs provided promising new insights into miR regulation [12,15], the construction and application of artificial synthetic circRNAs targeting specific onco-miRs remains limited.

miR-1269a is one of the most well-characterized onco-miRs and is overexpressed in several cancers [16–19]. Elevated expression of miR-1269a has been implicated in critical cancer-related processes, including proliferation, invasion, and apoptosis [17–19]. In the present study, we established a novel synthetic circRNA that carries miR-1269a binding sequences and investigated its potential application as a therapeutic tool to slow cancer progression.

## 2. Materials and Methods

### 2.1. Cell Culture

Human OSCC cell lines (Sa3, HSC3, HSC2, HSC4, and SAS) were purchased from the Japanese Collection of Research Bioresources Cell Bank (Ibaraki, Japan) and the RIKEN BioResource Center (Tsukuba, Japan). Short tandem repeat analysis by PCR amplification was performed for cell authentication. OSCC cells were cultured at 37 °C with 5% CO<sub>2</sub>.

### 2.2. Differential Expression of miR-1269a in the Cancer Genome Atlas (TCGA)

We used TCGA head and neck squamous cell carcinoma (HNSC) clinical data obtained from cBioportal (<https://www.cbioportal.org>, accessed on 10 April 2020). Among TCGA-HNSC, we selected OSCC samples whose primary sites were the alveolar ridge, buccal mucosa, floor of mouth, hard palate, lip, and tongue. A total of 297 OSCCs and 30 normal samples for which miR-1269a sequence data were available were retrieved from the TCGA data portal. Analysis of differential miR-1269a expression was performed according to the previous study [16].

### 2.3. qRT-PCR Analysis of miR-1269a Expression

Total RNA from the OSCC cell lines Sa3, HSC3, HSC2, HSC4, and SAS was extracted using a microRNA purification kit (Thermo Fisher Scientific, Waltham, MA, USA) and reverse-transcribed. Expression levels of miR-1269a were measured by qRT-PCR according to the previous study [16]. All qRT-PCR assays were performed in triplicate.

### 2.4. Luciferase Reporter Assays

A luciferase reporter vector (pmirGLO, Promega, Madison, WI, USA) containing the miR-1269a binding site (CCAGTAGCACCGACAGTCCAG) was constructed using *PmeI* and *XbaI* restriction enzymes (Figure 1C, Luc-1269a, Takara Bio, Inc., Kusatsu, Shiga, Japan). HEK293 cells ( $1.0 \times 10^4$  cells) were seeded in 96-well plates and co-transfected with Luc-



England Biolabs) and then with T4 polynucleotide kinase (New England Biolabs). Finally, the linear RNA was circularized using T4 RNA ligase (New England Biolabs).

#### 2.6. Confirmation of circRNA-1269a Synthesis

To verify the closed-loop structure of circRNA-1269a, reverse-transcribed cDNA was amplified using a TopTaq Master Mix kit (Qiagen, Germantown, MD, USA) with divergent or convergent primers. After reverse transcription, divergent primers (5'-AGGGCGAATTCCAGCACACTGGC-3' (sense) and 5'-CCAAGGAATCAAGGGCGAATTCTGCAGA-3' (antisense)) were used to amplify a DNA PCR fragment containing the head-to-tail circRNA junction point. Convergent primers (5'-GCGAATTGGGCCCTCTAGATGCATGCTC-3' (sense) and 5'-CACTAGTAACGGCCGCCAGTGTGCTG-3' (antisense)) were used to amplify a DNA PCR fragment containing 2 or 4 repeats of the miR-1269a binding sites. PCR products were then cloned and sequenced.

#### 2.7. Transfection of circRNA-1269a

SAS cells were seeded in 6-well plates at  $2.0 \times 10^5$  cells/well prior to transfection with 10 nM circRNA-1269a (2X or 4X) using Lipofectamine 3000 (Thermo Fisher Scientific), according to the manufacturer's instructions. The cells were incubated for 24–96 h and collected for subsequent functional experiments.

#### 2.8. Cell Proliferation Assay

Cellular proliferation assays to examine how circRNA-1269a affects cellular growth were conducted using circRNA-1269a-treated cells seeded in 60 mm dishes at  $1.0 \times 10^4$  viable cells/dish. The cells were counted using a Luna™ Automated Cell Counter (Logos Biosystems, Annandale, VA, USA) at 24 h intervals from 24 to 120 h.

#### 2.9. Migration Assay

To investigate how circRNA-1269a affects cellular migration, transfected cells were plated in 6-well culture plates in DMEM containing 10% FBS and cultured until confluence was achieved. A wound was created in the middle of each plate using a 200 µL micropipette tip. The plates were then incubated at 37 °C, 5% CO<sub>2</sub> in serum-free medium. Migration was visualized by measuring the area of the wound every 12 h using Lenaraf220b free software (<http://www.vector.co.jp/soft/dl/win95/art/se312811.html> (accessed on 10 April 2020)).

#### 2.10. Proteomic Analysis of the Effects of circRNA-1269a Treatment

After circRNA treatment, cells were harvested with a cell scraper, resuspended in 30 mL PBS, collected with two rounds of centrifugation, and stored at −80 °C until use. Data-independent acquisition (DIA) proteomic analysis was performed by Kazusa Genome Technologies, Inc. (Kisarazu, Japan) according to a previously reported method [20]. The threshold to define altered protein expression was  $\geq 2.0$ -fold change and  $p < 0.05$  (Welch's *t*-test) between the treated and untreated groups. The expression intensity values for proteins with significant differential expression were obtained using a fold-change cutoff  $\geq 2.0$  or  $\leq 0.5$  ( $p < 0.05$ ) and visualized by volcano plots [21].

#### 2.11. Gene Set Enrichment Analysis (GSEA)

GSEA was used to analyze the molecular pathways related to proteins with upregulated expression after circRNA-1269a treatment. The protein lists were uploaded into GSEA software (<https://www.gsea-msigdb.org/gsea/login.jsp> (accessed on 1 May 2022)) [22,23], and the Hallmark gene set in The Molecular Signatures Database was applied [23,24].

#### 2.12. Identification of miR-1269a Targets

The miR-1269a target genes were predicted based on the TargetScan Human database (Release 7.2, [http://www.targetscan.org/vert\\_72/](http://www.targetscan.org/vert_72/); accessed on 1 August 2019). We then compared the miR-1269a target genes and upregulated proteins to find the common targets

of miR-1269a. TCGA clinical data from cBioPortal (<https://www.cbioportal.org>; data downloaded on 12 June 2021) were used for Kaplan–Meier analyses of overall survival for common targets of miR-1269a. Gene expression grouping data for each gene were collected from OncoLnc (<http://www.oncolnc.org/>; accessed on 18 August 2021).

### 2.13. Analysis of PLCG2 in OSCC Patients

The clinical significance of PLCG2 was investigated using OSCC data among TCGA-HNSC (<https://tcga-data.nci.nih.gov/tcga/>; accessed on 12 June 2021; OSCC, 314 cases; Normal, 30 cases). Clinical parameters and gene expression data were obtained from cBioPortal (<http://www.cbioportal.org/>; accessed on 13 July 2019) [25,26] and OncoLnc (<http://www.oncolnc.org/>; accessed on 1 August 2019) [27]. Monovariate and multivariate analyses were also performed according to the previous study [16]. Multivariate analyses were performed by JMP Pro 15.0.0 (SAS Institute Inc., Cary, NC, USA).

### 2.14. Statistical Analyses

Welch's *t*-test assessed the comparisons between the treated and untreated groups. Dunnett's test assessed differences between multiple groups were compared with the control group. SPSS 20.0 was used for all statistical analyses, and  $p < 0.05$  was defined as a statistical significance cutoff. All experiments were repeated at least three times. Means  $\pm$  SEM are displayed as representative values in the figures.

## 3. Results

### 3.1. Expression Levels of miR-1269a in OSCC Patients in the TCGA Dataset and OSCC Cell Lines

The TCGA dataset showed that miR-1269a expression was significantly upregulated in OSCC tissues (N = 297) compared with normal counterparts (N = 30) (Figure 1A;  $p < 0.05$ ). We also used qRT-PCR to measure miR-1269a expression levels in different OSCC cell lines to determine the optimal line for subsequent functional assays (Figure 1B). The miR-1269a levels were highest in SAS cells, and this line was used for further studies.

### 3.2. Validation of a Specific Sequence for miR-1269a Sponge Function

We constructed a luciferase vector (Luc-1269a) containing a specific sequence that has a sponge function toward miR-1269a (Figure 1C). We confirmed this sponge function using HEK293 cells co-transfected with Luc-1269a and miR-1269a mimics. Luciferase activity of Luc-1269a co-transfected with miR-1269a mimics (50 or 100 nM) was significantly lower than that for control cells (0 nM), indicating that the specific sequence on Luc-1269a has a sponge function for miR-1269a (Figure 1D,  $p < 0.05$ ).

### 3.3. Construction and Verification of circRNA-1269a

RNA circularization was performed by enzymatic ligation using synthetic linear RNAs containing two or four miR-1269a binding sites (linearRNA-1269a) termed 2X and 4X miR-1269a, respectively (Figure 2A). After synthesis, RT-PCR and sequencing were used to verify the correct construction of circRNA-1269a. PCR products obtained using divergent primers were amplified from the end-to-end junction regions, whereas PCR products using convergent primers contained two or four miR-1269a binding sites (Figure 2A). RT-PCR results showed that both circRNA-1269a and linearRNA-1269a yielded the expected products when amplified using convergent primers (2X, 164 bp; 4X, 248 bp; Figure 2B and Figure S1). In contrast, divergent primers generated the expected products only for circRNA-1269a (Figure 2C and Figure S1; 123 bp). Moreover, Sanger sequencing of the PCR products using divergent primers confirmed the correct sequence in the end-to-end ligation junction of circRNA-1269a (Figure 2D).

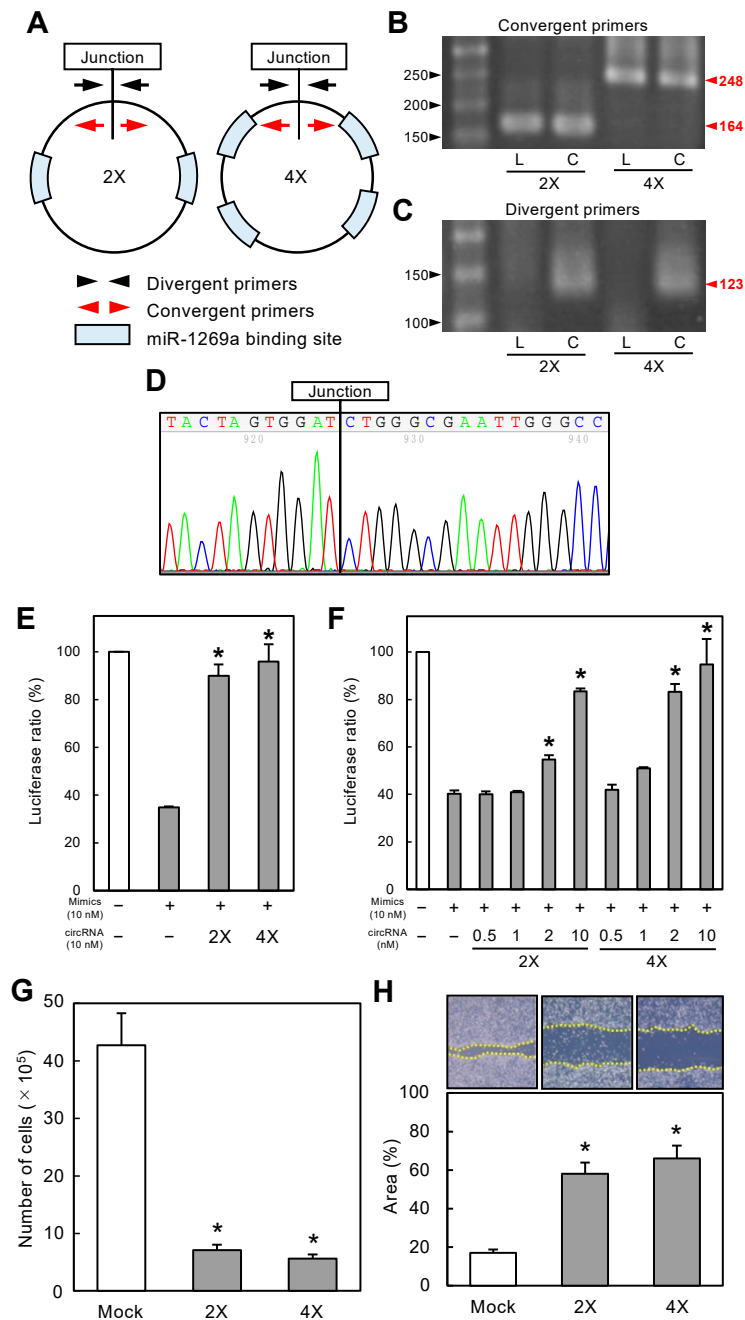


**Figure 2.** Construction of circRNA-1269a and its functional effects. (A) circRNA-1269a constructs, where 2X and 4X contain 2 and 4 repeats of miR-1269a binding sites, respectively. (B) Both linearRNA-1269a (L) and circRNA-1269a (C) yielded expected products when using convergent RT-PCR primers (2X, 164 bp; 4X, 248 bp). (C) Divergent primers generate the expected products in circRNA-1269a (C) (123 bp). (D) Sanger sequencing of the PCR products using divergent primers confirmed that circRNA-1269a has the correct end-to-end ligation junction. (E) Luciferase activity (Luc-1269a) in cells co-transfected with miR-1269a mimics and circRNA-1269a is significantly higher than for cells transfected with only miR-1269a mimics (\*,  $p < 0.05$ ). (F) Dose-dependent sponge function of circRNA-1269a. As the circRNA-1269a concentration increases, stimulatory effects on luciferase activity strengthen, with the maximal effect seen at 10 nM, the highest concentration tested (\*,  $p < 0.05$ ). (G) Cellular proliferation of circRNA-1269a-treated cells is significantly decreased relative to mock-treated cells 72 h after treatment (\*,  $p < 0.05$ ). (H) The wound area decreased significantly in circRNA-1269a-treated cells after 12 h compared with that for mock-treated cells (\*,  $p < 0.05$ ).

### 3.4. Functional Effects of Synthetic miR-1269a-Specific circRNA

To examine the functional capability of circRNA-1269a, normalized luciferase reporter assays (Firefly luciferase/Renilla luciferase activities) were conducted after co-transfection of cells with Luc-1269a, circRNA-1269a, and miR-1269a mimics. Successful activity of circRNA-1269a would involve a sponge function that counteracts the inhibitory effects of the miR-1269a mimics. Thus, we predicted that circRNA-1269a would preserve the luciferase activity of Luc-1269a by competitively binding to miR-1269a. The luciferase activity of Luc-1269a in cells co-transfected with miR-1269a mimics and circRNA-1269a was indeed significantly greater than in cells transfected with only miR-1269a mimics (Figure 2E,  $p < 0.05$ ). Moreover, these effects were dose-dependent. As the concentration of circRNA-1269a increased, the stimulatory effects on luciferase activity became stronger with a maximal effect at the highest concentration of 10 nM (Figure 2F,  $p < 0.05$ ). Thus, we used 10 nM circRNA-1269a for subsequent functional studies.

### 3.5. circRNA-1269a Inhibits Proliferation and Migration of OSCC Cells

To evaluate the effect of circRNA-1269a on cellular growth, we performed a cellular proliferation assay. We observed a significant decrease in proliferation of circRNA-1269a-treated cells compared with mock-treated cells (72 h after treatment; Figure 2G;  $p < 0.05$ ). The migration assay showed that the area of a wound created with a micropipette tip decreased significantly ( $p < 0.05$ ) in circRNA-1269a-treated cells after 12 h compared with mock-treated cells (Figure 2H,  $p < 0.05$ ).

### 3.6. Proteomic Analysis of circRNA-1269a-Treated OSCC Cells

miRs exert at least some effects on target mRNAs by altering their translation into proteins. To elucidate the mechanisms of circRNA-1269a, we performed protein expression analyses of DIA proteomics data collected from circRNA-1269a-treated and untreated (mock) cells. We identified 4729 individual proteins. Volcano plots of data for circRNA-1269a-treated cells show proteins having expression that was significantly ( $p < 0.05$ ) up-regulated (2X, 542 proteins; 4X, 458 proteins) or downregulated (2X, 351 proteins; 4X, 289 proteins) by more than two-fold (Figure 3A). Unsupervised hierarchical clustering of all expressed proteins showed a clear differential protein expression pattern for cells with circRNA-1269a treatment (Figure 3B). To identify the molecular pathways in OSCC cells that were affected by circRNA-1269a treatment, we performed gene set enrichment analysis (GSEA) using TCGA-HNSC RNA-seq data. GSEA analysis revealed that “apoptosis”, and particularly the apoptotic proteins caspase-3, -7, and -8, was the most enriched pathway in the circRNA-1269a-treated cells (Figure 3C–E;  $p < 0.05$ ). These results suggested that circRNA-1269a treatment contributes to an antitumor effect toward OSCC via an apoptosis pathway.

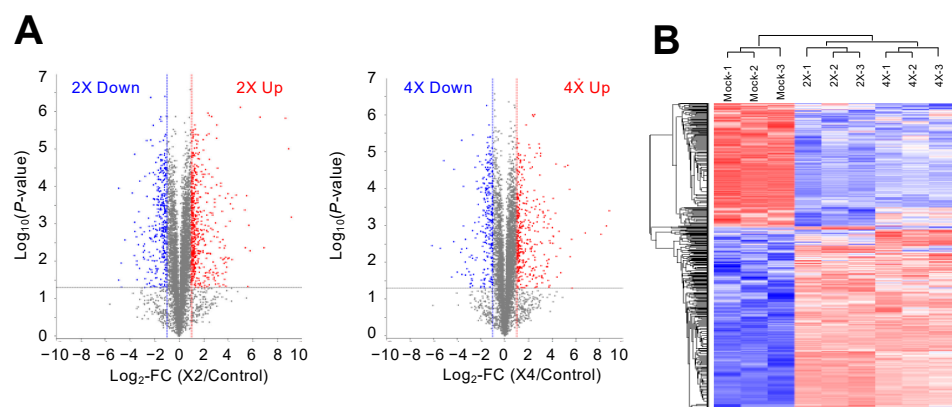
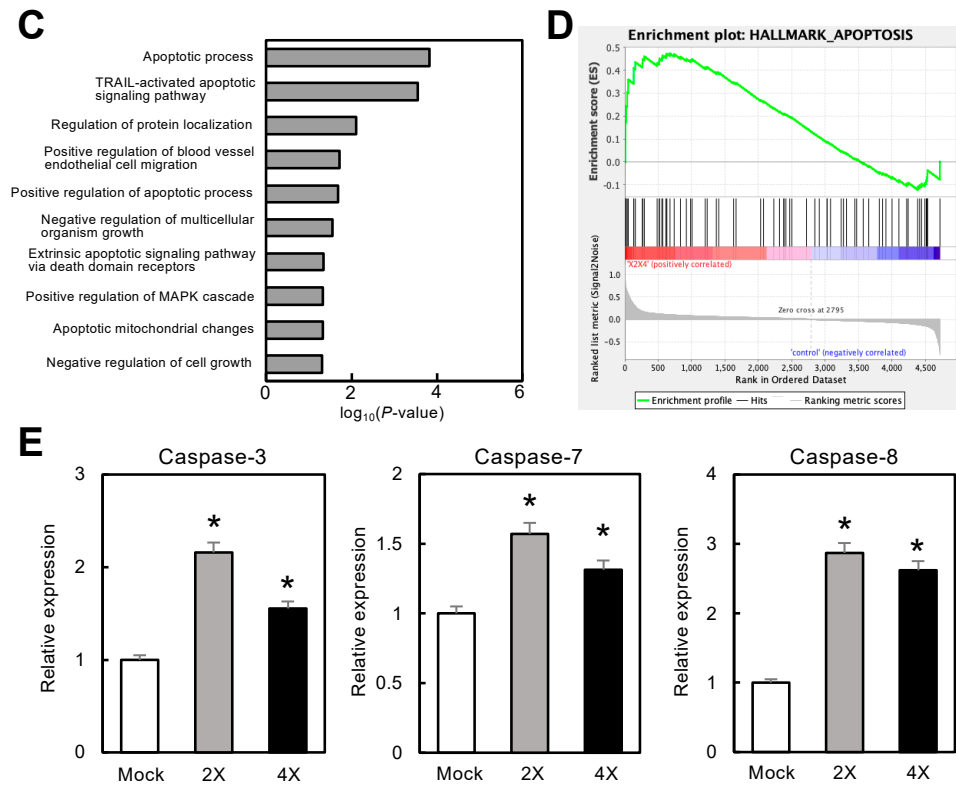


Figure 3. Cont.



**Figure 3.** Proteomic analysis of circRNA-1269a-treated OSCC cells. (A) Volcano plots of protein expression data from DIA proteomic analysis. The X- and Y-axis show the  $\log_2$ -fold change (FC) and  $\log_{10}$  ( $p$ -value), respectively. Blue points represent downregulated proteins with an absolute  $\log_2$ -FC <  $-2.0$ . Red points represent upregulated proteins with an absolute  $\log_2$ -FC >  $2.0$ . (B) Unsupervised hierarchical clustering of all expressed proteins shows a clear differential pattern for circRNA-1269a treatment. (C,D) GSEA using TCGA-HNSC RNA-seq data reveals that “apoptosis” is the most enriched pathway in the circRNA-1269a-treated group. (E) Overexpression of the apoptosis-related proteins caspase-3, -7, and -8 was observed after treatment with circRNA-1269a (\*,  $p < 0.05$ ).

### 3.7. Function of the circRNA-1269a Target Protein, PLCG2, in OSCC Patients

The strategy used to identify miR-1269a targets was summarized in Figure 4A. Based on a search of the TargetScan Human database (Release 7.2) for common putative target proteins, we found 2947 genes that had putative miR-1269a binding sites (Figure 4A). Furthermore, DIA proteomic analysis found 284 proteins containing putative miR-1269a binding sites in 2X and 4X circRNA-1269a-treated cells. A total of 50 putative target proteins were identified in both the proteomic analysis and the TargetScan Human database search (Table 1). We assessed these 50 proteins in terms of information for overall survival rate and expression levels in the TCGA database. We selected PLCG2 as a downstream target of circRNA-1269a (Figure 4A). PLCG2 was overexpressed in OSCC cells treated with circRNA-1269a (Figure 4B), suggesting that the circRNA-1269a/miR-1269a/PLCG2 axis is an important pathway in OSCC cells. In addition, the TCGA dataset showed that PLCG2 gene expression is significantly upregulated in OSCC tissues (N = 314) compared with healthy counterparts (N = 30) (Figure 4C;  $p < 0.05$ ). Cox proportional hazards regression analysis of PLCG2 expression was performed for 5-year overall survival rates (Figure 4D), PLCG2 gene expression level, disease stage, pathological grade, and patient age. The multivariate analysis showed that PLCG2 expression level was an independent prognostic factor (HR 0.6127,  $p < 0.05$ ; Figure 4E). These results indicated that PLCG2 has a tumor-suppressive function related to molecular pathogenesis and clinical prognosis in OSCC patients (Figure 4F).

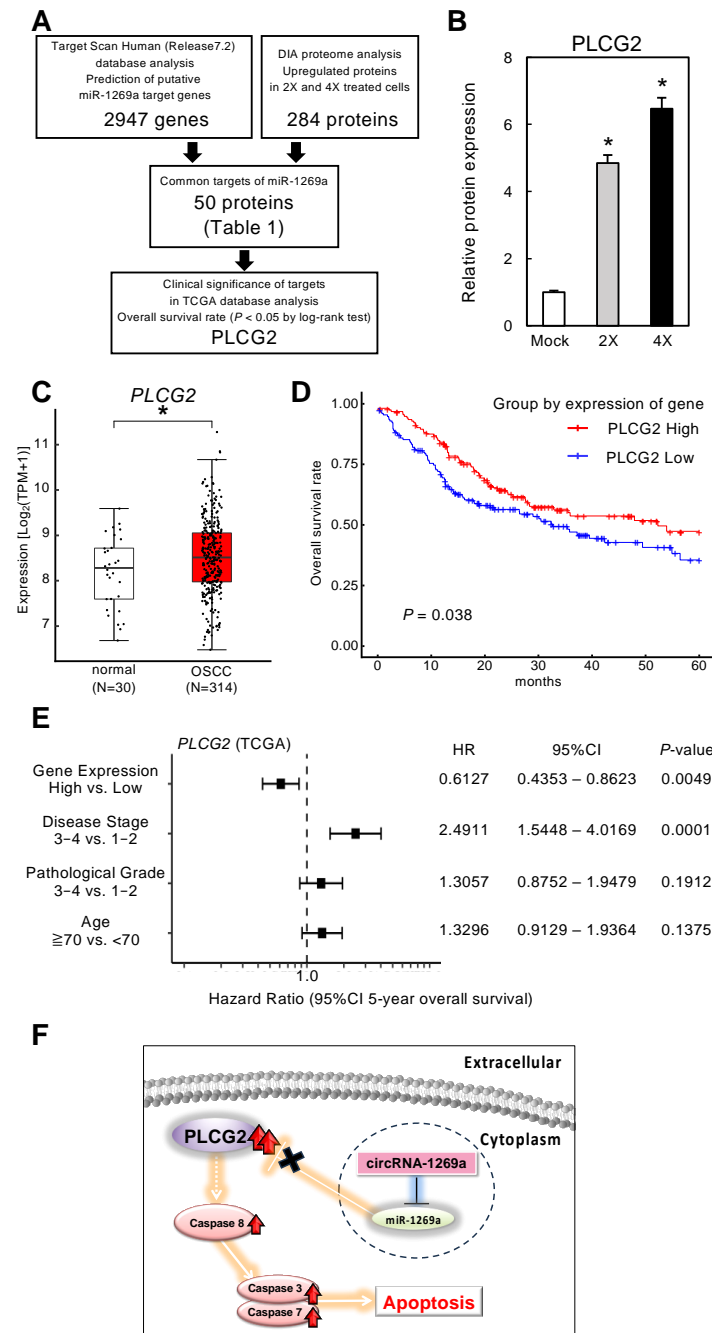


**Figure 4.** Function of the circRNA-1269a target, PLCG2, in OSCC patients. **(A)** A total of 2947 genes having a putative miR-1269a binding site were identified in a search of the TargetScan Human database (Release 7.2). In cells treated with 2X or 4X circRNA-1269a, 284 proteins were identified in a DIA proteomic analysis, and of these, 50 proteins were also identified in the TargetScan database search. These 50 proteins were assessed based on overall survival rate and expression levels in the TCGA database. PLCG2 was identified as a target protein of circRNA-1269a. **(B)** PLCG2 protein expression after circRNA-1269a treatment (\*,  $p < 0.05$ ). **(C)** Clinical significance of PLCG2 in OSCC clinical specimens determined by TCGA analysis (\*,  $p < 0.05$ ). **(D)** Kaplan–Meier curves of 5-year overall survival frequencies according to PLCG2 expression. **(E)** Forest plot showing results of multivariate analysis of PLCG2 identified by analysis of the TCGA-HNSC dataset (HR: hazard ratio; CI: confidence interval). **(F)** Schematic representation role of the circRNA-1269a/miR-1269a/PLCG2 axis that leads to apoptosis.

**Table 1.** Identification of common putative targets by TargetScan database and DIA proteomic analysis.

Protein Name	Symbol	Ave Ratio		p-Value
		2X	4X	
Calcium-binding and coiled-coil domain-containing protein 2	CALCOCO2	2.20	2.11	$2.68 \times 10^{-7}$
Collagen and calcium-binding EGF domain-containing protein 1	CCBE1	28.49	26.84	$3.41 \times 10^{-5}$
Cap-specific mRNA (nucleoside-2'-O-)-methyltransferase 1	CMTR1	2.64	2.19	$8.67 \times 10^{-7}$
Cytokine receptor-like factor 3	CRLF3	2.32	2.36	$1.25 \times 10^{-4}$
Deoxycytidine kinase	DCK	2.35	2.17	$1.44 \times 10^{-5}$
DCN1-like protein 5	DCUN1D5	2.20	2.04	$4.82 \times 10^{-7}$
Coagulation factor X	F10	72.09	87.02	$4.06 \times 10^{-6}$
Fibroblast growth factor 2	FGF2	2.63	2.85	$5.48 \times 10^{-7}$
Peptidyl-prolyl cis-trans isomerase FKBP4	FKBP4	2.50	2.20	$1.13 \times 10^{-6}$
Glucosamine 6-phosphate N-acetyltransferase	GNPNAT1	2.27	2.13	$3.88 \times 10^{-5}$
Interferon-induced protein with tetratricopeptide repeats 1	IFIT1	44.90	40.03	$5.39 \times 10^{-10}$
Interferon-induced protein with tetratricopeptide repeats 5	IFIT5	6.50	5.34	$9.78 \times 10^{-8}$
Interferon-related developmental regulator 1	IFRD1	2.07	2.00	$4.98 \times 10^{-8}$
Interleukin-1 receptor accessory protein-like 1	IL1RAPL1	2.98	3.30	$1.53 \times 10^{-2}$
tRNA N(3)-methylcytidine methyltransferase METTL2B	METTL2B	3.87	3.33	$3.88 \times 10^{-6}$
Neuron navigator 1	NAV1	4.05	4.22	$1.68 \times 10^{-2}$
U8 snoRNA-decapping enzyme	NUDT16	3.07	2.55	$6.66 \times 10^{-7}$
Partitioning defective 6 homolog beta	PARD6B	2.12	2.27	$1.32 \times 10^{-7}$
Protocadherin-7	PCDH7	2.04	2.15	$4.26 \times 10^{-3}$
Chronophin	PDXP	2.93	2.30	$3.78 \times 10^{-5}$
1-phosphatidylinositol 4,5-bisphosphate phosphodiesterase gamma-2	PLCG2	4.85	6.47	$3.81 \times 10^{-3}$
Pleckstrin homology domain-containing family B member 2	PLEKHB2	3.85	4.31	$1.16 \times 10^{-4}$
Phospholipid scramblase 1	PLSCR1	4.49	4.23	$2.25 \times 10^{-7}$
Purine nucleoside phosphorylase	PNP	2.44	2.37	$8.05 \times 10^{-7}$
Podocalyxin	PODXL	2.12	2.42	$4.34 \times 10^{-5}$
Amidophosphoribosyltransferase	PPAT	2.40	2.17	$6.02 \times 10^{-7}$
Proteasome assembly chaperone 1	PSMG1	2.44	2.04	$1.90 \times 10^{-6}$
Sulfhydryl oxidase 1	QSOX1	2.02	2.08	$1.32 \times 10^{-6}$
Ras-related protein Rab-43	RAB43	2.15	2.10	$2.17 \times 10^{-7}$
Serine/threonine-protein kinase RIO2	RIOK2	2.18	2.06	$4.80 \times 10^{-7}$
GTP-binding protein Rit1	RIT1	2.49	2.35	$7.59 \times 10^{-4}$
E3 ubiquitin-protein ligase RNF114	RNF114	2.35	2.30	$2.13 \times 10^{-4}$
RWD domain-containing protein 1	RWDD1	2.34	2.03	$1.63 \times 10^{-4}$
Deoxynucleoside triphosphate triphosphohydrolase SAMHD1	SAMHD1	8.28	6.54	$9.29 \times 10^{-8}$
GTP-binding protein SAR1a	SAR1A	2.61	2.33	$1.37 \times 10^{-5}$
Sodium-coupled neutral amino acid transporter 2	SLC38A2	2.17	2.29	$1.12 \times 10^{-4}$
Protein sprouty homolog 4	SPRY4	3.37	3.30	$7.71 \times 10^{-6}$
Signal transducer and activator of transcription 2	STAT2	2.49	2.21	$1.12 \times 10^{-5}$
Antigen peptide transporter 2	TAP2	2.04	2.09	$1.80 \times 10^{-6}$
Tax1-binding protein 1	TAX1BP1	5.42	5.74	$2.15 \times 10^{-9}$
Tumor necrosis factor receptor superfamily member 10A	TNFRSF10A	3.48	3.75	$1.50 \times 10^{-6}$
Tripartite motif-containing protein 14	TRIM14	2.18	2.10	$2.27 \times 10^{-6}$
E3 ubiquitin-protein ligase TRIM38	TRIM38	10.57	11.20	$1.19 \times 10^{-6}$
TSC22 domain family protein 2	TSC22D2	2.24	2.37	$5.14 \times 10^{-5}$
Thioredoxin-like protein 1	TXNL1	2.65	2.24	$1.90 \times 10^{-6}$

Table 1. Cont.

Protein Name	Symbol	Ave Ratio		p-Value
		2X	4X	
tRNA wybutosine-synthesizing protein 3 homolog	TYW3	2.55	2.24	$1.14 \times 10^{-4}$
Ubiquitin-associated and SH3 domain-containing protein B	UBASH3B	2.26	2.15	$4.69 \times 10^{-4}$
Ubiquitin/ISG15-conjugating enzyme E2 L6	UBE2L6	4.59	3.82	$2.30 \times 10^{-6}$
Ubiquitin thioesterase OTU1	YOD1	9.71	7.68	$1.37 \times 10^{-4}$
YrdC domain-containing protein, mitochondrial	YRDC	2.52	2.43	$7.59 \times 10^{-8}$

#### 4. Discussion

OSCC can have a poor prognosis and a high recurrence rate [28–31]. Although research on OSCC has advanced substantially, the five-year overall survival rate for this cancer remains below 50% [32]. Therefore, novel therapeutic targets for OSCC that act at a molecular level are needed. Numerous endogenous circRNAs are gaining increasing attention in cancers [13,33–35]. Several reports [13,33–35], including our previous study [13], showed that circRNAs are involved in the progression, metastasis, and multidrug resistance of cancers, suggesting that circRNAs could be diagnostic and/or therapeutic targets for multiple cancers. In addition, circRNAs have two characteristics, namely multiple miR binding sites that inhibit the function of the target miR and higher resistance to nuclease degradation relative to linear RNAs. Therefore, we hypothesized that synthetic circRNAs, which have been designed to function as exogenous miR inhibitors, would show promise for molecular cancer therapy [36].

In the present study, we selected miR-1269a as the target of newly developed synthetic circRNAs. Our previous data revealed that miR-1269a is upregulated in head and neck SCCs [16]. miR-1269a also promotes tumor progression and acts as an onco-miR in lung and gastric cancers, leading to the inhibition of apoptosis [17–19]. Based on our previously determined specific binding sequence for miR-1269a (Figure 1), we constructed an artificial synthetic circRNA that includes the miR-1269a binding sequence (circRNA-1269a) and that was circularized by novel enzymatic ligation (Figure 2). We confirmed that circRNA-1269a indeed has a sponge function for miR-1269a (Figure 2) and investigated downstream functions of miR-1269a in OSCC cells treated with circRNA-1269a. Our data demonstrated that circRNA-1269a inhibited cell proliferation and migration of the OSCC cell line by competitive inhibition of miR-1269a activity (Figure 2). Gene Ontology and GSEA of DIA proteomics data showed that circRNA-1269a treatment promotes apoptosis (Figure 3). In addition, our search of the TargetScan database identified PLCG2, which is involved in various biological processes including cell proliferation, cell migration, and apoptosis, as a target molecule of circRNA1269a/miR-1269a (Figure 4). Similar to previous reports showing that overexpression of PLCG2 occurs in gastric cancer, lymphoma, and hepatocytes [37–40] and that increased phosphorylation of p38 and JNK leads to apoptosis [40], our data here demonstrated overexpression of PLCG2 and marked enhancement of caspase-3, -7, and -8 expression in OSCC cells treated with circRNA-1269a, thus confirming that PLCG2 may enhance apoptosis in OSCCs. p38 and JNK signaling pathways are two important intracellular signaling pathways that are known to be tightly associated with apoptosis [41,42]. Caspase-8 is the most upstream component in the caspase cascade [43,44]. Meanwhile, caspase-3 and -7 are downstream effectors of the two apoptotic pathways and cleave various cytoplasmic and nuclear substrates including DNA fragmentation factor and DNA-dependent protein kinase [45,46].

Although a circRNA delivery system for OSCC regions is required, these data suggest that circRNA-1269a/miR-1269a could act as a potential therapeutic axis for OSCCs. We also demonstrated that circRNA-1269a-induced activation of PLCG2 and its downstream pathways may be involved in these biological processes. Our confirmation

that circRNA-1269a/miR-1269a/PLCG2 can inhibit OSCC proliferation and migration by promoting apoptosis in OSCC cells in vitro indicates that PLCG2 overexpression via the circRNA-1269a/miR-1269a axis may be a valuable tool for controlling OSCC growth (Figure 4F). These findings further establish that the design and construction of efficient artificial synthetic circRNAs represents a novel strategy to achieve miR loss-of-function in molecular cancer therapeutics and could have potential future therapeutic applications for cancers.

## 5. Conclusions

These results suggest that synthetic circRNA-1269a inhibits tumor progression via effects on miR-1269a and its downstream targets, indicating that artificial circRNAs could represent an effective OSCC therapeutic.

**Supplementary Materials:** The following supporting information can be downloaded at: <https://www.mdpi.com/article/10.3390/jpm14030330/s1>, Figure S1: Original image of agarose gel electrophoresis. A, original image of Figure 2B; B, original image of Figure 2C.

**Author Contributions:** Project administration, A.K. and K.U.; conducted experiments, A.K., N.S., J.M. and K.U.; biochemical analyses, A.K., R.N., K.K., T.S. and C.M.; data analysis, R.N., K.K., T.S. and C.M.; wrote the manuscript, A.K., N.S., J.M. and K.U. All authors have read and agreed to the published version of the manuscript.

**Funding:** This work was supported by JSPS KAKENHI, grant number JP22H03286 (A. Kasamatsu). J. Moss was supported by the Intramural Research Program, National Institutes of Health, National Heart, Lung, and Blood Institute.

**Institutional Review Board Statement:** Not applicable.

**Informed Consent Statement:** Not applicable.

**Data Availability Statement:** All relevant data are within the paper.

**Acknowledgments:** We thank Kikuo Takahashi for kindly providing detailed information for the SAS cells; Hideyuki Kodama and Toshiaki Ando for technical assistance; and JAM Post (<https://www.jamp.com/svcs/> (accessed on 10 January 2024)) for proofreading this paper. The results shown here are in part based upon data generated by the TCGA Research Network: <https://www.cancer.gov/tcga> (accessed on 10 April 2020).

**Conflicts of Interest:** The authors declare no conflicts of interest.

## References

1. Bartel, D.P. *MicroRNAs: Target Recognition and Regulatory Functions*; Elsevier: Amsterdam, The Netherlands, 2009; Volume 136, pp. 215–233.
2. Farazi, T.A.; Spitzer, J.I.; Morozov, P.; Tuschl, T. MiRNAs in Human Cancer. *J. Pathol.* **2011**, *223*, 102–115. [[CrossRef](#)] [[PubMed](#)]
3. Ventura, A.; Jacks, T. MicroRNAs and Cancer: Short RNAs Go a Long Way. *Cell* **2009**, *136*, 586–591. [[CrossRef](#)] [[PubMed](#)]
4. Selaru, F.M.; Olaru, A.V.; Kan, T.; David, S.; Cheng, Y.; Mori, Y.; Yang, J.; Paun, B.; Jin, Z.; Agarwal, R.; et al. MicroRNA-21 Is Overexpressed in Human Cholangiocarcinoma and Regulates Programmed Cell Death 4 and Tissue Inhibitor of Metalloproteinase 3. *Hepatology* **2009**, *49*, 1595–1601. [[CrossRef](#)] [[PubMed](#)]
5. Liu, X.; Meltzer, S.J. Gastric Cancer in the Era of Precision Medicine. *Cell. Mol. Gastroenterol. Hepatol.* **2017**, *3*, 348–358. [[CrossRef](#)] [[PubMed](#)]
6. Memczak, S.; Jens, M.; Elefsinioti, A.; Torti, F.; Krueger, J.; Rybak, A.; Maier, L.; Mackowiak, S.D.; Gregersen, L.H.; Munschauer, M.; et al. Circular RNAs Are a Large Class of Animal RNAs with Regulatory Potency. *Nature* **2013**, *495*, 333–338. [[CrossRef](#)]
7. Chen, L.-L. The Biogenesis and Emerging Roles of Circular RNAs. *Nat. Rev. Mol. Cell Biol.* **2016**, *17*, 205–211. [[CrossRef](#)]
8. Jeck, W.R.; Sharpless, N.E. Detecting and Characterizing Circular RNAs. *Nat. Biotechnol.* **2014**, *32*, 453–461. [[CrossRef](#)]
9. Wang, Z.; Ma, K.; Pitts, S.; Cheng, Y.; Liu, X.; Ke, X.; Kovaka, S.; Ashktorab, H.; Smoot, D.T.; Schatz, M.; et al. Novel Circular RNA CircNF1 Acts as a Molecular Sponge, Promoting Gastric Cancer by Absorbing MiR-16. *Endocr. Relat. Cancer* **2019**, *26*, 265–277. [[CrossRef](#)]
10. Liu, H.; Bi, J.; Dong, W.; Yang, M.; Shi, J.; Jiang, N.; Lin, T.; Huang, J. Correction to: Invasion-Related Circular RNA CircFNDC3B Inhibits Bladder Cancer Progression through the MiR-1178-3p/G3BP2/SRC/FAK Axis. *Mol. Cancer* **2020**, *19*, 124. [[CrossRef](#)]
11. Huang, B.; Zhou, D.; Huang, X.; Xu, X.; Xu, Z. Silencing CircSLC19A1 Inhibits Prostate Cancer Cell Proliferation, Migration and Invasion through Regulating MiR-326/MAPK1 Axis. *Cancer Manag. Res.* **2020**, *12*, 11883–11895. [[CrossRef](#)]

12. Hansen, T.B.; Jensen, T.I.; Clausen, B.H.; Bramsen, J.B.; Finsen, B.; Damgaard, C.K.; Kjems, J. Natural RNA Circles Function as Efficient MicroRNA Sponges. *Nature* **2013**, *495*, 384–388. [[CrossRef](#)]
13. Ando, T.; Kasamatsu, A.; Kawasaki, K.; Hiroshima, K.; Fukushima, R.; Iyoda, M.; Nakashima, D.; Endo-Sakamoto, Y.; Uzawa, K. Tumor Suppressive Circular RNA-102450: Development of a Novel Diagnostic Procedure for Lymph Node Metastasis from Oral Cancer. *Cancers* **2021**, *13*, 5708. [[CrossRef](#)] [[PubMed](#)]
14. Chen, L.; Zhang, S.; Wu, J.; Cui, J.; Zhong, L.; Zeng, L.; Ge, S. CircRNA\_100290 Plays a Role in Oral Cancer by Functioning as a Sponge of the MiR-29 Family. *Oncogene* **2017**, *36*, 4551–4561. [[CrossRef](#)] [[PubMed](#)]
15. Han, D.; Li, J.; Wang, H.; Su, X.; Hou, J.; Gu, Y.; Qian, C.; Lin, Y.; Liu, X.; Huang, M.; et al. Circular RNA CircMTO1 Acts as the Sponge of MicroRNA-9 to Suppress Hepatocellular Carcinoma Progression. *Hepatology* **2017**, *66*, 1151–1164. [[CrossRef](#)]
16. Oshima, S.; Asai, S.; Seki, N.; Minemura, C.; Kinoshita, T.; Goto, Y.; Kikkawa, N.; Moriya, S.; Kasamatsu, A.; Hanazawa, T.; et al. Identification of Tumor Suppressive Genes Regulated by MiR-31-5p and MiR-31-3p in Head and Neck Squamous Cell Carcinoma. *Int. J. Mol. Sci.* **2021**, *22*, 6199. [[CrossRef](#)]
17. Bu, P.; Wang, L.; Chen, K.-Y.; Rakhilin, N.; Sun, J.; Closa, A.; Tung, K.-L.; King, S.; Kristine Varanko, A.; Xu, Y.; et al. MiR-1269 Promotes Metastasis and Forms a Positive Feedback Loop with TGF- $\beta$ . *Nat. Commun.* **2015**, *6*, 6879. [[CrossRef](#)]
18. Hu, Y.; Dingerdissen, H.; Gupta, S.; Kahsay, R.; Shanker, V.; Wan, Q.; Yan, C.; Mazumder, R. Identification of Key Differentially Expressed MicroRNAs in Cancer Patients through Pan-Cancer Analysis. *Comput. Biol. Med.* **2018**, *103*, 183–197. [[CrossRef](#)]
19. Gan, T.-Q.; Tang, R.-X.; He, R.-Q.; Dang, Y.-W.; Xie, Y.; Chen, G. Upregulated MiR-1269 in Hepatocellular Carcinoma and Its Clinical Significance. *Int. J. Clin. Exp. Med.* **2015**, *8*, 714–721.
20. Kawashima, Y.; Nagai, H.; Konno, R.; Ishikawa, M.; Nakajima, D.; Sato, H.; Nakamura, R.; Furuyashiki, T.; Ohara, O. Single-Shot 10K Proteome Approach: Over 10,000 Protein Identifications by Data-Independent Acquisition-Based Single-Shot Proteomics with Ion Mobility Spectrometry. *J. Proteome Res.* **2022**, *21*, 1418–1427. [[CrossRef](#)] [[PubMed](#)]
21. Uzawa, K.; Amelio, A.L.; Kasamatsu, A.; Saito, T.; Kita, A.; Fukamachi, M.; Sawai, Y.; Toeda, Y.; Eizuka, K.; Hayashi, F.; et al. Resveratrol Targets Urokinase-Type Plasminogen Activator Receptor Expression to Overcome Cetuximab-Resistance in Oral Squamous Cell Carcinoma. *Sci. Rep.* **2019**, *9*, 12179. [[CrossRef](#)] [[PubMed](#)]
22. Mootha, V.K.; Lindgren, C.M.; Eriksson, K.-F.; Subramanian, A.; Sihag, S.; Lehar, J.; Puigserver, P.; Carlsson, E.; Ridderstråle, M.; Laurila, E.; et al. PGC-1 $\alpha$ -Responsive Genes Involved in Oxidative Phosphorylation Are Coordinately Downregulated in Human Diabetes. *Nat. Genet.* **2003**, *34*, 267–273. [[CrossRef](#)]
23. Subramanian, A.; Tamayo, P.; Mootha, V.K.; Mukherjee, S.; Ebert, B.L.; Gillette, M.A.; Paulovich, A.; Pomeroy, S.L.; Golub, T.R.; Lander, E.S.; et al. Gene Set Enrichment Analysis: A Knowledge-Based Approach for Interpreting Genome-Wide Expression Profiles. *Proc. Natl. Acad. Sci. USA* **2005**, *102*, 15545–15550. [[CrossRef](#)] [[PubMed](#)]
24. Liberzon, A.; Subramanian, A.; Pinchback, R.; Thorvaldsdóttir, H.; Tamayo, P.; Mesirov, J.P. Molecular Signatures Database (MSigDB) 3.0. *Bioinformatics* **2011**, *27*, 1739–1740. [[CrossRef](#)] [[PubMed](#)]
25. Gao, J.; Aksoy, B.A.; Dogrusoz, U.; Dresdner, G.; Gross, B.; Sumer, S.O.; Sun, Y.; Jacobsen, A.; Sinha, R.; Larsson, E.; et al. Integrative Analysis of Complex Cancer Genomics and Clinical Profiles Using the CBioPortal. *Sci. Signal.* **2013**, *6*, pl1. [[CrossRef](#)] [[PubMed](#)]
26. Cerami, E.; Gao, J.; Dogrusoz, U.; Gross, B.E.; Sumer, S.O.; Aksoy, B.A.; Jacobsen, A.; Byrne, C.J.; Heuer, M.L.; Larsson, E.; et al. The CBio Cancer Genomics Portal: An Open Platform for Exploring Multidimensional Cancer Genomics Data. *Cancer Discov.* **2012**, *2*, 401–404. [[CrossRef](#)] [[PubMed](#)]
27. Anaya, J. OncoLnc: Linking TCGA Survival Data to MRNAs, MiRNAs, and LncRNAs. *PeerJ Comput. Sci.* **2016**, *2*, e67. [[CrossRef](#)]
28. Baba, T.; Sakamoto, Y.; Kasamatsu, A.; Minakawa, Y.; Yokota, S.; Higo, M.; Yokoe, H.; Ogawara, K.; Shiiba, M.; Tanzawa, H.; et al. Persephin: A Potential Key Component in Human Oral Cancer Progression through the RET Receptor Tyrosine Kinase-Mitogen-Activated Protein Kinase Signaling Pathway. *Mol. Carcinog.* **2015**, *54*, 608–617. [[CrossRef](#)] [[PubMed](#)]
29. Kita, A.; Kasamatsu, A.; Nakashima, D.; Endo-Sakamoto, Y.; Ishida, S.; Shimizu, T.; Kimura, Y.; Miyamoto, I.; Yoshimura, S.; Shiiba, M.; et al. Activin B Regulates Adhesion, Invasiveness, and Migratory Activities in Oral Cancer: A Potential Biomarker for Metastasis. *J. Cancer* **2017**, *8*, 2033–2041. [[CrossRef](#)]
30. Yamamoto, A.; Kasamatsu, A.; Ishige, S.; Koike, K.; Saito, K.; Kouzu, Y.; Koike, H.; Sakamoto, Y.; Ogawara, K.; Shiiba, M.; et al. Exocyst Complex Component Sec8: A Presumed Component in the Progression of Human Oral Squamous-Cell Carcinoma by Secretion of Matrix Metalloproteinases. *J. Cancer Res. Clin. Oncol.* **2013**, *139*, 533–542. [[CrossRef](#)]
31. Wang, L.; Zhang, Y.; Xie, F. T-Regulatory Cell/T Helper 17 Cell Imbalance Functions as Prognostic Biomarker of Oral Squamous Cell Carcinoma—CONSORT. *Medicine* **2020**, *99*, e23145. [[CrossRef](#)]
32. Sim, Y.C.; Hwang, J.-H.; Ahn, K.-M. Overall and Disease-Specific Survival Outcomes Following Primary Surgery for Oral Squamous Cell Carcinoma: Analysis of Consecutive 67 Patients. *J. Korean Assoc. Oral Maxillofac. Surg.* **2019**, *45*, 83–90. [[CrossRef](#)]
33. Vo, J.N.; Cieslik, M.; Zhang, Y.; Shukla, S.; Xiao, L.; Zhang, Y.; Wu, Y.-M.; Dhanasekaran, S.M.; Engelke, C.G.; Cao, X.; et al. The Landscape of Circular RNA in Cancer. *Cell* **2019**, *176*, 869–881.e13. [[CrossRef](#)]
34. Patop, I.L.; Kadener, S. CircRNAs in Cancer. *Curr. Opin. Genet. Dev.* **2018**, *48*, 121–127. [[CrossRef](#)]
35. Szabo, L.; Salzman, J. Detecting Circular RNAs: Bioinformatic and Experimental Challenges. *Nat. Rev. Genet.* **2016**, *17*, 679–692. [[CrossRef](#)]
36. Liu, X.; Abraham, J.M.; Cheng, Y.; Wang, Z.; Wang, Z.; Zhang, G.; Ashktorab, H.; Smoot, D.T.; Cole, R.N.; Boronina, T.N.; et al. Synthetic Circular RNA Functions as a MiR-21 Sponge to Suppress Gastric Carcinoma Cell Proliferation. *Mol. Ther. Nucleic Acids* **2018**, *13*, 312–321. [[CrossRef](#)]

37. Zhang, B.; Wu, Q.; Ye, X.-F.; Liu, S.; Lin, X.-F.; Chen, M.-C. Roles of PLC-Gamma2 and PKCalpha in TPA-Induced Apoptosis of Gastric Cancer Cells. *World J. Gastroenterol.* **2003**, *9*, 2413–2418. [[CrossRef](#)]
38. Graham, D.B.; Robertson, C.M.; Bautista, J.; Mascarenhas, F.; Diacovo, M.J.; Montgrain, V.; Lam, S.K.; Cremasco, V.; Dunne, W.M.; Faccio, R.; et al. Neutrophil-Mediated Oxidative Burst and Host Defense Are Controlled by a Vav-PLCgamma2 Signaling Axis in Mice. *J. Clin. Investig.* **2007**, *117*, 3445–3452. [[CrossRef](#)] [[PubMed](#)]
39. Shearn, C.T.; Reigan, P.; Petersen, D.R. Inhibition of Hydrogen Peroxide Signaling by 4-Hydroxynonenal Due to Differential Regulation of Akt1 and Akt2 Contributes to Decreases in Cell Survival and Proliferation in Hepatocellular Carcinoma Cells. *Free Radic. Biol. Med.* **2012**, *53*, 1–11. [[CrossRef](#)] [[PubMed](#)]
40. Chen, X.; Lv, Q.; Ma, J.; Liu, Y. PLCγ2 Promotes Apoptosis While Inhibits Proliferation in Rat Hepatocytes through PKCD/JNK MAPK and PKCD/P38 MAPK Signalling. *Cell Prolif.* **2018**, *51*, e12437. [[CrossRef](#)] [[PubMed](#)]
41. Kuo, W.-H.; Chen, J.-H.; Lin, H.-H.; Chen, B.-C.; Hsu, J.-D.; Wang, C.-J. Induction of Apoptosis in the Lung Tissue from Rats Exposed to Cigarette Smoke Involves P38/JNK MAPK Pathway. *Chem. Biol. Interact.* **2005**, *155*, 31–42. [[CrossRef](#)] [[PubMed](#)]
42. Mansouri, A.; Ridgway, L.D.; Korapati, A.L.; Zhang, Q.; Tian, L.; Wang, Y.; Siddik, Z.H.; Mills, G.B.; Claret, F.X. Sustained Activation of JNK/P38 MAPK Pathways in Response to Cisplatin Leads to Fas Ligand Induction and Cell Death in Ovarian Carcinoma Cells. *J. Biol. Chem.* **2003**, *278*, 19245–19256. [[CrossRef](#)] [[PubMed](#)]
43. Reed, J.C.; Pellecchia, M. Apoptosis-Based Therapies for Hematologic Malignancies. *Blood* **2005**, *106*, 408–418. [[CrossRef](#)] [[PubMed](#)]
44. Coutinho-Camillo, C.M.; Lourenço, S.V.; Nishimoto, I.N.; Kowalski, L.P.; Soares, F.A. Caspase Expression in Oral Squamous Cell Carcinoma. *Head Neck* **2011**, *33*, 1191–1198. [[CrossRef](#)] [[PubMed](#)]
45. Derfuss, T.; Fickenscher, H.; Kraft, M.S.; Henning, G.; Lengenfelder, D.; Fleckenstein, B.; Meinel, E. Antiapoptotic Activity of the Herpesvirus Saimiri-Encoded Bcl-2 Homolog: Stabilization of Mitochondria and Inhibition of Caspase-3-like Activity. *J. Virol.* **1998**, *72*, 5897–5904. [[CrossRef](#)]
46. Casciola-Rosen, L.A.; Anhalt, G.J.; Rosen, A. DNA-Dependent Protein Kinase Is One of a Subset of Autoantigens Specifically Cleaved Early during Apoptosis. *J. Exp. Med.* **1995**, *182*, 1625–1634. [[CrossRef](#)]

**Disclaimer/Publisher’s Note:** The statements, opinions and data contained in all publications are solely those of the individual author(s) and contributor(s) and not of MDPI and/or the editor(s). MDPI and/or the editor(s) disclaim responsibility for any injury to people or property resulting from any ideas, methods, instructions or products referred to in the content.